Distributed Control and Optimization in DC Microgrids

Jinxin Zhao [a] Florian Dörfler [b]

[a] *Department of Mechanical and Aerospace Engineering, University of California, Los Angeles, California, 90024*

[b] *Automatic Control Laboratory, Swiss Federal Institute of Technology (ETH) Zürich, Switzerland, 8092*

Abstract

Due to their compatibility with renewable and distributed generation, microgrids are a promising operational architecture for future power systems. Here we consider the operation of DC microgrids that arise in many applications. We adopt a linear circuit model and propose a decentralized voltage droop control strategy that is inspired by frequency droop control in AC networks. We demonstrate that our primary droop control strategy is able to achieve fair and stable load sharing (even in presence of actuation constraints) or an economic dispatch of the generation formulated as a quadratic and linearly-constrained optimization problem on the source injections. Similar to frequency droop control, voltage droop control induces a steady-state voltage drift depending on the imbalance of load and generation in the microgrid. To compensate for this steady-state error, we consider two secondary control strategies. A purely decentralized secondary integral control strategy successfully compensates for the steady-state voltage drifts yet it fails to achieve the desired optimal steady-state injections. Next, we propose a consensus filter that requires communication among the controllers, that regulates the voltage drift, and that recovers the desired optimal injections. The performance and robustness of our controllers are illustrated through simulations.

1 Introduction

Driven by environmental concerns, renewable energy sources are rapidly deployed, such as photovoltaic and wind generation. These sources will, for the most part, be deployed as small-scale generation units in low-voltage distribution networks. As a natural consequence, the conventional centralized and hierarchical operation of power grids is advancing towards distributed and flat architectures, and so-called microgrids have been proposed as conceptual solutions. Microgrids are low-voltage electrical distribution networks, composed of distributed generations, storages and loads. The advantages of microgrids are as follows: First, microgrids are capable of connecting to the power transmission grid, but they are also able to island themselves and operate independently, e.g., in case of an outage. Second, microgrids can be deployed as stand-alone small-footprint power systems (possibly in remote locations) while providing high quality power supply, e.g., in hospitals, research facilities, and school campuses. Third and finally, microgrids are naturally designed to integrate small-scale distributed generation, i.e., power is generated where it is needed without transmission losses.

Microgrids have been proposed based on either alternative current (AC) or direct current (DC) paradigms. AC power grids have been in service for many decades, and their components and operation are well understood. The operational paradigms from conventional AC power transmission networks have been inherited in AC microgrids [2]. However, using DC microgrids has the following advantages: there is an increasing number of DC sources and storages (e.g., solar cells and Li-ion batteries), end-user equipment (e.g., electric vehicles), and most of the contemporary electronic appliances. In [3] it is demonstrated that most of the loads supplied by AC nowadays can operate also with a DC supply. In comparison to AC microgrids with DC sources, the efficiency is raised since conversion losses of DC-to-AC inverters are removed — though conversion losses arise in DC-to-DC converters for sources with different voltage levels. Finally, DC microgrids are widely deployed in aircrafts and spacecrafts [4]. In summary, DC microgrids are a promising technology that has already attracted much research attention.

Literature review: The articles [2,5,6] focus on the hardware implementation of DC microgrids. A hierarchical control layout for DC microgrids is proposed in [2]: a primary controller rapidly stabilizes the grid, and a secondary controller (on a slower time scale) corrects for the steady-state error induced by primary control. An experimental system involving solar-cell, wind turbine and power storage is designed and constructed in [5]. A

⋆ A preliminary version of part of this paper's results is [1].

Email addresses: jinxinzh@ucla.edu (Jinxin Zhao), dorfler@ethz.ch (Florian Dörfler).

low-voltage DC distribution system for sensitive loads is described in [6]. In [7], a modeling method of DC microrid clusters is described. A scenario-based operation strategy for a DC microgrid is developed in [8], emphasizing the detailed model and control of wind turbine and battery. Feasibility conditions for DC micorgrids with constant power loads were proposed in [9]. A cooperative control paradigm is proposed in [10] to establish a distributed primary/secondary control framework for DC microgrids with communication capabilities. Distributed controllers have been studied to regulate multiterminal DC transmission systems which share similar problem aspects with DC microgrids. The controller proposed in [11] achieves fair power sharing and asymptotically minimizes the cost of the power injections. Distributed controllers focusing on voltage control are studied in [12,13]. In [14] a unified port-Hamitonian system model is proposed, and the performance of decentralized PI control is discussed for a multi-terminal DC transmission system. For AC microgrids a flat and distributed operation architecture has been proposed in [15,16], consisting simultaneous (without time-scale separation) primary, secondary, and tertiary control. Inspired by these AC operation strategies we seek similar solutions for DC microgrids.

Contribution and contents: In this article, we propose a comprehensive operational control strategy for DC microgrids in order to achieve multiple objectives.

In Section 2, we introduce the considered DC microgrid model. Inspired by the shortcomings of conventional DC droop control and the merits of frequency droop control in AC systems, we propose a novel primary voltage droop control strategy in Section 3. Our proposed primary control strategy is fully decentralized, and we demonstrate that it is capable of stabilizing the grid while achieving load sharing and avoiding actuator saturation. As base scenario we consider a purely resistive network with constant current loads, but we also discuss extensions to other load and network models. In Section 4, we consider the economic dispatch of multiple generating units and formulate it as a convex optimization problem. We demonstrate that the set of minimizers of the economic dispatch are in one-to-one correspondence with the steady states achieved by our primary voltage droop control with appropriately chosen control gains. As a result, we propose a selection of control gains (droop coefficients) to achieve economic optimality in decentralized way and without a model of the network or the loads. In Section 5, we discuss the limitations of droop control causing steady-state voltage drifts, and we study secondary control strategies to compensate for it. First, we consider fully decentralized integral controllers and illustrate their limitations. Next, we propose a distributed consensus filter that relies on communication between local controllers. We show that this distributed control strategy is capable of regulating the voltage drifts while simultaneously achieving tertiary-level objectives such as load sharing or economic dispatch. In Section 6, we present simulation results to illustrate the performance and robustness of our primary and secondary controllers. Finally Section 7 concludes the paper.

Aside from the importance of DC microgrids in their own right, we sincerely believe that the considered DC scenario also serves as valuable and accessible introduction to many power system operational paradigms that have nonlinear and complex parallels in AC networks.

Preliminaries and Notation

Vectors and matrices: Let $\mathbb{1}_n$ and $\mathbb{0}_n$ be the n-dimensional vectors of unit and zero entries, respectively. Let $\mathbf{I_n} \in \mathbb{R}^{n\times n}$ be the n-dimensional identity. Let $\mathbf{diag}(v)$ represent a diagonal matrix with the elements of v on the diagonal. For a symmetric matrix $A = A^T$, the notation $A > 0$, $A \geq 0$, $A < 0$, and $A \leq 0$ means that A is positive definite, positive semidefinite, and negative definite and negative semidefinite, respectively.

Algebraic graph theory: Consider a connected, undirected, and weighted graph $G = (\mathcal{V}, \mathcal{E}, W)$, where $\mathcal{V} = \{1, ...n\}$ is the set of nodes, $\mathcal{E} \subset \mathcal{V} \times \mathcal{V}$ is the set of undirected edges, and $W = W^T \in \mathbb{R}^{n\times n}$ is the adjacency matrix with entries $w_{ij} > 0$, if $(i, j) \in \mathcal{E}$ and $w_{ij} = 0$ otherwise. The degree matrix $D \in \mathbb{R}^{n\times n}$ is the diagonal matrix with elements $d_{ii} = \sum_{j=1,j\neq i}^{n} w_{ij}$. The Laplacian matrix $L = L^T \in \mathbb{R}^{n\times n}$ is defined by $L = D - W$, and it satisfies $L \geq 0$ and $L\mathbf{1_n} = \mathbf{0_n}$. If the graph is connected, then the null space of L is spanned by $\mathbf{1_n}$, and all the other $n - 1$ eigenvalues of L are strictly positive.

2 DC Microgrid Model

For our purposes, a microgrid is a linear connected circuit with associated undirected graph $G(\mathcal{V}, \mathcal{E}, W)$, nodes $\mathcal{V} = \{1, ..., n\}$, and edges $\mathcal{E} \subset \mathcal{V} \times \mathcal{V}$. We assume that all lines in the DC microgrid are purely resistive, and refer to Remark 3.1 for an extension of our results of more general line impedances. The adjacency matrix W is defined with nozero entries $w_{ij} = w_{ji} = 1/R_{ij}$ for $(i, j) \in \mathcal{E}$, where R_{ij} is the resistance of the line connecting nodes $i, j \in \mathcal{V}$. The diagonal degree matrix $D \in \mathbb{R}^{n\times n}$ has elements $d_{ii} = \sum_{j=1,j\neq i}^{n} w_{ij}$. The admittance matrix Y is defined as $Y = D - W$. Thus, $Y = Y^T \in \mathbb{R}^{n\times n}$ is a real-valued Laplacian matrix satisfying $\mathbb{1}_n^T Y = \mathbb{0}_n^T$.

We partition the set of nodes into m sources and $n - m$ loads: $\mathcal{V} = \mathcal{V}_S \cup \mathcal{V}_L$. Throughout this paper we denote sources and loads by the superscripts S and L, respectively. The sources are assumed to be controllable current sources with positive current injections $I_i^S \geq 0$ and are assembled in the vector I^S. Each source is constrained by its output current capacity $\bar{I}_i$, i.e.,

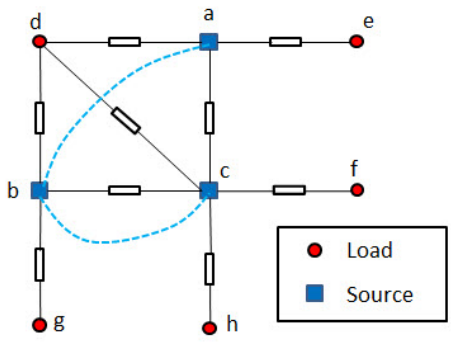

Fig. 1. A DC Microgrid with three sources and five loads. The blue dashed lines indicate the communication among the secondary controllers (29) that we design in Section 5.

$I_i^S \in [0, \bar{I}_i]$. The loads are assumed to be constant-current loads with negative current injections $I_i^L \leq 0$ and are assembled in the vector I^L. Following Kirchhoff's and Ohm's laws, the network model is built as [1]

$$\begin{bmatrix} I^S \\ I^L \end{bmatrix} = \begin{bmatrix} Y_{SS} & Y_{SL} \\ Y_{SL}^T & Y_{LL} \end{bmatrix} \begin{bmatrix} V^S \\ V^L \end{bmatrix} \tag{1}$$

where the admittance matrix Y is partitioned according to sources and loads, and V^S and V^L represent the nodal voltages (potentials) of sources and loads, respectively. Since Y is a Laplacian matrix, $\mathbb{1}_n^T Y = \mathbb{0}_n^T$ and a necessary feasibility condition for equation (1) is

$$\mathbb{1}_m^T I^S + \mathbb{1}_{n-m}^T I^L = 0. \tag{2}$$

Fig. 1 shows an example network of a DC microgrid.

In this DC microgrid setup, we assume that source buses are controllable voltage sources and load buses are passive current sinks. [2] The control objectives are (i) balancing of generation and load (as in (2)) (ii) in a stable fashion and (iii) subject to fair resource allocation (e.g., a fair load sharing), (iv) subject to possible actuation constraints (e.g., within source capacity limits), and (v) subject to load voltages within pre-described bounds. In this article, we show that the control objectives (i)-(iv) can be achieved in a plug-and-play fashion, that is, without knowledge of the system model and data and in a distributed way without centralized coordination. We return to the control objective (v) in Remark 5.1.

[1] Loads in DC power systems are conventionally modeled as constant-current, constant-impedance, constant-voltage or constant-power loads [3]. Often loads do not belong to a single category but display a combination of the above properties. We mainly focus on pure constant-current loads which arise primarily in electronic loads and also in some conventional loads such as LED lighting. We find that these loads are the mathematically most challenging linear loads. In Remarks 3.2 and 3.3 we show how all our results extend to constant-impedance loads and constant-voltage buses.

[2] This setup includes the case when a current load is attached to a source bus whose terminal voltage is controllable.

3 Primary Droop Control & Load Sharing

We briefly review *frequency droop control* in AC microgrids [2] to motivate our proposed control strategy for DC microgrids. In AC microgrids the active power injection P_i at source i is controlled to be proportional to its frequency deviation $\dot{\theta}_i$ (from a nominal frequency) as

$$P_i = P_i^* - C_i \dot{\theta}_i, \tag{3}$$

where the control gain $C_i > 0$ is referred to as the droop coefficient, $P_i^* \in [0, \bar{P}_i]$ is a nominal injection setpoint, and $\bar{P}_i$ is the capacity of source i. For a particular selection of droop coefficients, it can be shown that frequency droop control stabilizes the AC microgrid to a synchronous solution and achieves proportional load sharing at steady state [16], that is, every source i injects active power P_i according its capacity $\bar{P}_i$: $P_i/\bar{P}_i = P_j/\bar{P}_j$ for all sources $i, j \in \mathcal{V}_S$. A key feature of AC frequency droop control is that it synthesizes the synchronous frequency as a global variable indicating the load/generation imbalance in the microgrid [15,16].

As for AC systems, a primary objective in DC microgrids is to synthesize local decentralized droop controllers that achieve *proportional load sharing* in the sense that

$$I_i^S/\bar{I}_i = I_j^S/\bar{I}_j \quad \text{for all } i, j \in \mathcal{V}_S\,, \tag{4}$$

where $I_i^S \in [0, \bar{I}_i]$ is the current injection of source $i \in \mathcal{V}_S$ and $\bar{I}_i > 0$ is its capacity. The conventional *DC voltage-vs-current droop controller* is given by (see [14,10,7])

$$I_i^S = I_i^* - C_i V_i^S, \tag{5}$$

where $I_i^* \in [0, \bar{I}_i]$ is an injection setpoint and the gain $C_i > 0$ is referred to as *droop coefficient*. Unless non-local (distributed or decentralized) secondary controllers or carefully tuned virtual impedance controllers are added, the control (5) does generally not achieve load sharing (especially for non-negligible line impedances); see [10] for a review. From a mathematical perspective this shortcoming is essentially due to the absence of a global variable such as the AC frequency.

Here we start from the observation that the conventional controller (5) can be interpreted as the steady-state of the following proportional-integral droop controller:

$$I_i^S = I_i^* - C_i \dot{V}_i^S - p_i\,, \tag{6a}$$
$$\dot{p}_i = C_i \dot{V}_i^S\,, \tag{6b}$$

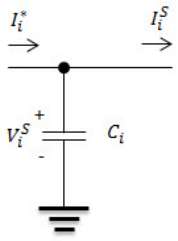

Fig. 2. Realization of droop control (7) as analog circuit

Observe that (6a) mimics the AC frequency droop (3) and (6b) is an integral controller compensating for steady-state drifts similar to a decentralized secondary frequency integral controller often added to droop in AC systems. Inspired by this observation, the success of frequency droop control (3) in AC systems, and the limitation of conventional DC droop control (5), we propose the *primary voltage droop controller*

$$I_i^S = I_i^* - C_i \dot{V}_i^S \,. \tag{7}$$

Fig. 2 shows an analog circuit realization of the droop controller (7) via a constant current source I_i^* and a shunt capacitor C_i reminiscent of shunt compensation in DC power systems [17]. The proposed primary droop control (7) is a fully decentralized local proportional control strategy. In a digital implementation, each generating unit is controlled as a voltage source with terminal voltage V_i^S, and a micro-controller realizes the droop (7) based on measurement of the output current I_i^S.

Similar to AC droop control (3), our controller (7) induces a global variable, namely a constant voltage drift, that depends on the load/generation imbalance: $\sum_{i\in\mathcal{V}_S} I_i^* + \sum_{j\in\mathcal{V}_L} I_j^L$. Of course, this drift has to be compensated by a secondary controller, which will be done in Section 5. Before that we analyze the primary droop control loop (1) and (7) by itself and show, among others, that it achieves stable proportional load sharing:

Theorem 3.1 (Primary control & load sharing) Consider the closed-loop droop-controlled microgrid (1) and (7). Then the following statements hold:
(1) Voltage drifts: all voltages V_i^S, $i \in \mathcal{V}_S$ converge exponentially to $V(t) = V^* + \dot{v}_{\text{drift}} t \cdot \mathbb{1}_m$, where $V^* \in \mathbb{R}^m$ is a constant vector and the common voltage drift is

$$\dot{v}_{\text{drift}} = \frac{\sum_{j\in\mathcal{V}_S} I_j^* + \sum_{j\in\mathcal{V}_L} I_j^L}{\sum_{j\in\mathcal{V}_S} C_j} \,. \tag{8}$$

(2) Proportional load sharing: if the droop coefficients and nominal injection setpoints are selected proportionally, that is, for all $i, j \in \mathcal{V}_S$

$$C_i/\bar{I}_i = C_j/\bar{I}_j \quad \text{and} \quad I_i^*/\bar{I}_i = I_j^*/\bar{I}_j, \tag{9}$$

then at steady state the load is shared proportionally.

Proof 3.1 *The closed-loop state space model* (1), (7) *is*

$$\begin{bmatrix} C\dot{V}^S \\ 0 \end{bmatrix} = \begin{bmatrix} I_S^* \\ I^L \end{bmatrix} - \begin{bmatrix} Y_{SS} & Y_{SL} \\ Y_{SL}^T & Y_{LL} \end{bmatrix} \begin{bmatrix} V^S \\ V^L \end{bmatrix} , \tag{10}$$

where $C = \boldsymbol{diag}(C_1, ..., C_m)$. *Since* Y_{LL} *is invertible [18, Lemma II.1], we eliminate the variable* $V^L = Y_{LL}^{-1}(I^L - Y_{SL}^T V^S)$. *from the second block of (algebraic) equations in* (10). *This elimination process, termed Kron-reduction in circuit theory [18], gives the Kron-reduced system*

$$\dot{V}^S = -C^{-1}\tilde{L}V^S + C^{-1}\tilde{I} \tag{11}$$

where $\tilde{I} = I_S^* - Y_{SL}Y_{LL}^{-1}I^L$ *and* $\tilde{L} = Y_{SS} - Y_{SL}Y_{LL}^{-1}Y_{SL}^T$ *is again a positive semidefinite Laplacian [18, Lemma II.1] with a unique zero eigenvalue. By Sylvester's Law of Inertia [19, Corollary 3], because* $C^{-1} > 0$ *and* $\tilde{L}$ *is symmetric,* $C^{-1}\tilde{L}$ *has the same number of negative, zero and positive eigenvalues as* $\tilde{L}$. *Thus,* $C^{-1}\tilde{L}$ *has one zero-eigenvalue and all other eigenvalues are positive. It follows that all modes of the Kron-reduced system* (11) *exponentially decay to zero with exception of the zero mode with right eigenvector* $\mathbb{1}_m$ *and left eigenvector* $C\mathbb{1}_m$. *This zero mode is integrated and all components of the vector* $\dot{V}_S$ *will exponentially converge to the same value* $\dot{v}_{\text{drift}}$. *We project the differential-algebraic equations* (10) *onto the zero mode by summing all equations* (10) *as* $\mathbb{1}_m^T C\dot{V}_S = \mathbb{1}_m^T I^S + \mathbb{1}_{n-m}^T I^L$. *In steady state for* $\dot{V}_S = \dot{v}_{\text{drift}}\mathbb{1}_m$, *we recover the voltage drift* (8). *Since* $\dot{V}_S(t)$ *converges exponentially to the constant* $\dot{v}_{\text{drift}}\mathbb{1}_m$, *we have that* $V(t)$ *converges exponentially to* $V^* + \dot{v}_{\text{drift}} t \cdot \mathbb{1}_m$, *where* $V^* \in \mathbb{R}^m$ *This proves statement (1).*

At steady state, the closed-loop injections are

$$I_i^S = -C_i \dot{v}_{\text{drift}} + I_i^* . \tag{12}$$

Thus, $I_i^S/\bar{I}_i = (-C_i\dot{v}_{\text{drift}} + I_i^*)/\bar{I}_i$. *The proportional load sharing objective* $I_i^S/\bar{I}_i = I_j^S/\bar{I}_j$ *(for all* $i, j \in \mathcal{V}_S$*) can be achieved by choosing* I_i^* *and* C_i *proportionally as in* (9). *This proves statement (2) of Theorem 3.1.* □

Theorem 3.1 gives a criterion for stable load sharing of the closed-loop system (1), (7), namely the droop coefficients need to be picked proportional to capacity $C_i = \gamma\bar{I}_i$, where $\gamma > 0$ is constant. Observe that Theorem 3.1 does not guarantee that the injections satisfy the actuation constraint $I_i \in [0, \bar{I}_i]$. If the control gains are chosen as in (9), then the actuation constraint is met if and only if the total load $\sum_{j\in\mathcal{V}_L} I_j^L$ can be satisfied by the maximal injections (at capacity) $\sum_{i\in\mathcal{V}_S} \bar{I}_i$.

Theorem 3.2 (Actuation constraints) Consider a stationary solution of the closed-loop system (1) and (7) with droop coefficients and setpoints chosen proportionally as in (9). The following statements are equivalent:

(1) Injection constraints: $0 \leq I_i^S \leq \bar{I}_i$ for all $i \in \mathcal{V}_S$;
(2) Load satisfiability: $\sum_{i\in\mathcal{V}_S} \bar{I}_i \geq -\sum_{j\in\mathcal{V}_L} I_j^L \geq 0$.

Proof 3.2 *The steady-state injections are given by* (8),(12). *The condition* $I_i^S \geq 0$, *for* $i \in \mathcal{V}_S$, *translates to*

$$I_i^S = I_i^* - C_i \frac{\sum_{j\in\mathcal{V}_S} I_j^* + \sum_{k\in\mathcal{V}_L} I_k^L}{\sum_{j\in\mathcal{V}_S} C_j} \geq 0.$$

For proportional coefficients (9), *we have* $C_i/I_i^* = C_j/I_j^*$ *and the previous inequality equivalently reads as*

$$\sum\nolimits_{k\in\mathcal{V}_L} I_k^L \leq -\sum\nolimits_{j\in\mathcal{V}_S} \left(I_j^* - C_j \frac{I_i^*}{C_i} \right) = 0.$$

A similar calculation, for $I_i^S \leq \bar{I}_i$, *for* $i \in \mathcal{V}_S$, *yields*

$$I_i^S = I_i^* - C_i \frac{\sum_{j\in\mathcal{V}_S} I_j^* + \sum_{k\in\mathcal{V}_L} I_k^L}{\sum_{j\in\mathcal{V}_S} C_j} \leq \bar{I}_i.$$

The coefficients satisfy $C_i/(\sum_{j\in\mathcal{V}_j} C_j) = \bar{I}_i/(\sum_{j\in\mathcal{V}_j} \bar{I}_j) = I_i^*/(\sum_{j\in\mathcal{V}_j} I_j^*)$, *thus the previous inequality also reads as*

$$\sum_{k\in\mathcal{V}_L} I_k^L \geq (I_i^* - \bar{I}_i) \frac{\sum_{j\in\mathcal{V}_j} C_j}{C_i} - \sum_{j\in\mathcal{V}_j} I_j^* = -\sum_{j\in\mathcal{V}_S} \bar{I}_j.$$

These inequalities complete the proof of Theorem 3.2.□

We conclude that the primary droop controller (7) achieves stable proportional load sharing in a fully decentralized way and while respecting actuation constraints. However, as in AC systems, the droop controller (7) induces a steady-state voltage drift (8) which is proportional to the total injection imbalance $\sum_{i\in\mathcal{V}_S} I_i^* + \sum_{j\in\mathcal{V}_L} I_j^L$. Notice that the total injection imbalance is zero (and hence $\dot{v}_{\text{drift}} = 0$) only if a precise forecast of the total load $\sum_{j\in\mathcal{V}_L} I_j^L$ is known and the nominal injections I_i^* can be scheduled accordingly. Such a precise forecast is generally not available, the nominal injections are fixed (typically to 0 or $\bar{I}_i$), and the loads are changing with time. Another way to reduce the voltage drift $\dot{v}_{\text{drift}}$ in (8) is to choose large droop coefficients C_i. On the other hand, the latter choice results in slow response of the system.

We will explicitly address the regulation of the voltage drift in Section 5. Before that we turn to the *tertiary control* (or energy management) problem (in Section 4) as well as extensions to other load and line models.

Remark 3.1 (Extension to Π-model) *Consider a microgrid with resistive-capacitive lines (e.g., underground cables) described by the* Π*-model [20] illustrated in Fig. 3. In this case, the DC microgrid model is given by*

$$\begin{bmatrix} I^S \\ I^L \end{bmatrix} = \begin{bmatrix} Y_{SS} & Y_{SL} \\ Y_{SL}^T & Y_{LL} \end{bmatrix} \begin{bmatrix} V^S \\ V^L \end{bmatrix} + C_d \begin{bmatrix} \dot{V}^S \\ \dot{V}^L \end{bmatrix} \tag{13}$$

where C_d *is a diagonal matrix with the shunt capacities as diagonal elements, i.e.,* $C_d = \boldsymbol{diag}(C_{d1}, ..., C_{dn})$.

The primary droop controller analogously regulates the microgrid and results in voltage drifts. This can be seen by substituting the droop controller $I^S = I^* - C\dot{V}^S$ *into* (13), *then the closed-loop state space equation is*

$$\left(C_d + \begin{bmatrix} C & 0 \\ 0 & 0 \end{bmatrix} \right) \begin{bmatrix} \dot{V}^S \\ \dot{V}^L \end{bmatrix} = \begin{bmatrix} I^* \\ I^L \end{bmatrix} - \begin{bmatrix} Y_{SS} & Y_{SL} \\ Y_{SL}^T & Y_{LL} \end{bmatrix} \begin{bmatrix} V^S \\ V^L \end{bmatrix}. \tag{14}$$

Since the model (14) *has the same structure as the Kron-reduced system* (11), *analogous arguments as in the proof of Theorem 3.1 show that all voltage drifts exponentially converge to the common constant value*

$$\dot{v}_{\text{drift}} = \frac{\sum_{j\in\mathcal{V}_S} I_j^* + \sum_{j\in\mathcal{V}_L} I_j^L}{\sum_{j\in\mathcal{V}_S} C_j + C_{d,j} + \sum_{j\in\mathcal{V}_L} C_{d,j}}.$$

All subsequent developments are analogous for the more detailed model (14) *and we focus on the model* (1), (7).□

Remark 3.2 *(***Extension to constant-impedance loads)** *Consider a DC microgrid with additional constant resistive loads (arising, e.g., in electric lighting and heating devices [3]), as shown in Fig. 4. We assume that there is at least one resistive load, we let* $R_j > 0 \in \mathbb{R}$ *be the impedance of load* j, *and we define the associated shunt admittance as* $Y_{\text{shunt},j} = 1/R_j$ *(which is zero if* $R_j = 0$*). The resulting current balance equations* (1) *are*

$$\begin{bmatrix} I^S \\ I^L \end{bmatrix} = \begin{bmatrix} Y_{SS} & Y_{SL} \\ Y_{SL}^T & Y_{LL} + Y_{\text{shunt}} \end{bmatrix} \begin{bmatrix} V^S \\ V^L \end{bmatrix}, \tag{15}$$

where $Y_{\text{shunt}} = \mathbf{diag}([1/R_1, ..., 1/R_{n-m}])$. *After implementing voltage droop control* (7) *at the source nodes and*

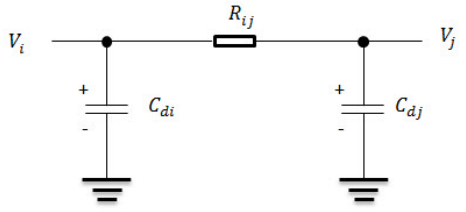

Fig. 3. Π-model with resistive series and capacitive shunt impedances

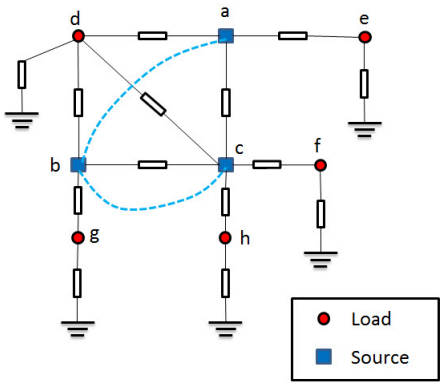

Fig. 4. Microgrid with impedance loads

applying Kron reduction, the closed-loop system is

$$C\dot{V}^S = -[Y_{SS} - Y_{SL}(Y_{LL} + Y_{\text{shunt}})^{-1}Y_{SL}^T]V^S + [I^* - Y_{SL}(Y_{LL} + Z_{LL})^{-1}I^L]. \quad (16)$$

Since the admittance matrix in (15) *is positive semidefinite and irreducibly diagonal dominant, we conclude that it is nonsingular [21, Corollary 6.2.27] and thus also positive definite. Since the class of positive definite matrices is closed under the Schur complement [22, Chapter 4], it follows that the Schur complement* $(Y_{SS} - Y_{SL}(Y_{LL} + Z_{LL})^{-1}Y_{SL}^T)$ *in* (16) *is positive definite. Hence, the system* (16) *is Hurwitz, and the states converge to the constant steady state* $[Y_{SS} - Y_{SL}(Y_{LL} + Z_{LL})^{-1}Y_{SL}^T]^{-1}[I^* - Y_{SL}(Y_{LL} + Z_{LL})^{-1}I^L]$ *without voltage drift.*

In conclusion, a DC microgrid with constant resitive loads is stabilized by fully decentralized voltage droop control (7)*. Essentially, the loads absorb any injections from the sources. We will not further pursue this model.* □

Remark 3.3 *(***Extension to constant-voltage buses***)* *Consider a DC microgrid with constant-voltage buses arising, e.g., in controllable electronic loads (chips), points-of-common coupling (PCCs), and substations. For notational simplicity, assume that all load buses have constant voltages* V^L *in* (1) *(our reasoning easily extends to a more general case). After implementing voltage droop control* (7)*, we obtain*

$$C\dot{V}^S = -Y_{SS}V^S + (I^* - Y_{SL}V^L) \quad (17a)$$
$$I^L = Y_{SL}^T V^S + Y_{LL}V^L. \quad (17b)$$

Since $Y_{SS} > 0$*, the system* (17a) *is Hurwitz, and* V^S *converges to the vector* $V^S(\infty) = Y_{SS}^{-1}(I^* - Y_{SL}V^L)$*. Thus, droop control stabilizes a microgrid with constant-voltage buses. We will not further pursue this model.* □

4 Optimal Economic Dispatch & Droop Control

The proportional choice of droop coefficients (9) leads to fair load sharing (4) among the sources proportional to their capacity. However, this objective may not be desirable when the sources rely on different energy generation and conversion mechanisms. For example, solar cells have lower capacities compared with diesel generators, but they may be preferred due to economic and environmental reasons. In the following, we consider an alternative generation dispatch criterion, namely the *economic dispatch* formalized as the optimization problem

$$\underset{\{u,\, V^S,\, V^L\}}{\text{minimize}} \; f(u) = \sum_{i=1}^m \frac{1}{2}\alpha_i u_i^2 \quad (18a)$$
$$\text{subject to} \begin{bmatrix} I_S^* + u \\ I^L \end{bmatrix} = Y \begin{bmatrix} V^S \\ V^L \end{bmatrix} \quad (18b)$$

The optimization problem (18) is convex with quadratic objective and linear constraints. The coefficients $\alpha_i > 0$ is chosen based on the marginal cost of power source i reflecting its fuel and operation costs , capacity, or other preferences. In case that the nominal injection setpoints I_i^* are zero, the decision variable u_i equals the total generation of source i. For nonzero setpoints $I_i^* > 0$, u_i is the reserve generation to meet the real-time demand.

Theorem 4.1 (Economic dispatch) Consider the optimization problem (18). The optimal injections are

$$u_i^* = -c/\alpha_i, \quad i \in \mathcal{V}_s\,, \quad (19)$$

where $c = \frac{\mathbb{1}_m^T I_S^* + \mathbb{1}_{n-m}^T I^L}{\sum_i 1/\alpha_i}$ is a constant.

Proof 4.1 *The Lagrangian associated to* (18) *is*

$$\mathcal{L}(u, V, \lambda) = \sum_{i=1}^m \frac{1}{2}\alpha_i u_i^2 + \lambda^T \left(\begin{bmatrix} I_S^* + u \\ I^L \end{bmatrix} - YV \right)$$

where $V = \begin{bmatrix} V^S \\ V^L \end{bmatrix}$ *and* $\lambda = \begin{bmatrix} \lambda^S \\ \lambda^L \end{bmatrix} \in \mathbb{R}^n$.

The KKT conditions $\frac{\partial \mathcal{L}}{\partial V} = 0$, $\frac{\partial \mathcal{L}}{\partial \lambda} = 0$ *and* $\frac{\partial \mathcal{L}}{\partial u} = 0$ *are necessary and sufficient for optimality due to the convexity of* (18) *[23] . The first condition is* $\frac{\partial \mathcal{L}}{\partial V} = -\lambda^T Y = 0$*. Since* Y *is a Laplacian matrix,* $\text{null}(Y) = \text{span}(\mathbb{1}_n)$*. Thus, we have that* $\lambda = c\mathbb{1}_n$*, where* $c \in \mathbb{R}$ *is a constant. The second condition is* $\frac{\partial \mathcal{L}}{\partial u} = u^T \mathbf{diag}(\alpha_i) + \lambda_S^T = 0$*. It follows that* $u_i^* = -c/\alpha_i$*. The constraint* (18b) *implies*

$$\mathbb{1}_n^T \begin{bmatrix} I_S^* + u \\ I^L \end{bmatrix} = \mathbb{1}_m^T I_S^* + \mathbb{1}_{n-m}^T I^L + \mathbb{1}_m^T u = \mathbb{1}_n^T YV = 0.$$

Since $u_i^* = -c/\alpha_i$*, then* $c\sum 1/\alpha_i = (\mathbb{1}_m^T I_S^* + \mathbb{1}_m^T I^L)$. □

Theorem 4.1 gives the optimal injections u_i as a function of the nominal injections I_S^*, the (possibly unknown)

loads I^L, and the cost coefficients α_i. Observe from (19) that at optimality all marginal costs are identical:

$$\alpha_i u_i^* = \alpha_j u_j^* \quad i \in \mathcal{V}_s \,. \tag{20}$$

Note the similarity between the optimal injections (19) and the steady-state injections of droop-controlled microgrid (8) and (12). Based on this observation, we present the following result: the optimal solution of the economic dispatch (19) can be achieved by appropriately designed droop controllers (7). Conversely, any steady state of the droop-controlled microgrid (1) and (7) is the optimal solution of the economic dispatch (19) with appropriately chosen parameters.

Corollary 4.1 (Droop control & economic dispatch) Consider the following two injections:
(**1**) The optimal injection $I_i^* + u_i^*$ of the economic dispatch problem (18) with cost coefficients α_i; and
(**2**) The steady-state injections $I_i^* - C_i \dot{v}_{\text{drift}}$ of the droop-controlled microgrid (1) and (7) with droop coefficients C_i.

These two injections are identical if and only if

$$\alpha_i C_i = \alpha_j C_j \quad \text{for all } i, j \in \mathcal{V}_S. \tag{21}$$

Proof 4.2 *In the economic dispatch optimization problem* (18)*, the unique optimal injection is*

$$I_i^* + u_i = I_i^* - \frac{1}{\alpha_i} \frac{\mathbb{1}_m^T I_S^* + \mathbb{1}_{n-m}^T I^L}{\sum_{j \in \mathcal{V}_S} \frac{1}{\alpha_j}}. \tag{22}$$

The stationary injection induced by droop-control is

$$I_i^* - C_i \dot{v}_{\text{drift}} = I_i^* - C_i \frac{\sum_{j \in \mathcal{V}_S} I_j^* + \sum_{k \in \mathcal{V}_L} I_k^L}{\sum_{j \in \mathcal{V}_S} C_j}. \tag{23}$$

First, observe that (22) *and* (23) *are equal when substituting $C_i = \beta/\alpha_i$ into* (23)*, where $\beta \in \mathbb{R}$ is constant. Conversely, if* (22) *and* (23) *are equal for all $i \in \mathcal{V}_S$, i.e.,*

$$I_i^* - \frac{1}{\alpha_i} \frac{\mathbb{1}_m^T I_S^* + \mathbb{1}_{n-m}^T I^L}{\sum_{j \in \mathcal{V}_S} \frac{1}{\alpha_j}} = I_i^* - C_i \frac{\sum_{j \in \mathcal{V}_S} I_j^* + \sum_{k \in \mathcal{V}_L} I_k^L}{\sum_{j \in \mathcal{V}_S} C_j},$$

it follows for every $i \in \mathcal{V}_S$ that $\sum_{i \in \mathcal{V}_S} C_i / \sum_{i \in \mathcal{V}_S} \frac{1}{\alpha_i} = \alpha_i C_i$. Since the left-hand side of this equality is constant for every $i \in \mathcal{V}_S$, we have $\alpha_i C_i = \alpha_j C_j$ for all $i, j \in \mathcal{V}_S$.□

Notice that the optimal injection (in the sense of the economic dispatch (18)) can be achieved in a fully decentralized manner, without any communication among the sources or a knowledge of the microgrid and the loads when the droop gains are chosen as $C_i = \beta/\alpha_i$ for some constant $\beta > 0$. In general, the optimal droop gain $D_i = \beta/\alpha_i$ and the droop gain $D_i = \gamma \bar{I}_i$ for proportional load sharing (satisfying the conditions (9)) are not identical unless $\alpha_i = c/\bar{I}_i$ for some constant $c \in \mathbb{R}$. We conclude that the economic dispatch (18) is a more versatile objective that includes load sharing (4) as a special case.

Finally, we remark that the proposed voltage droop controllers are designed to be optimal with respect to a (terminal) steady-state cost, but they are decentralized and independent of the system model and the load profile. Provided that detailed and accurate model data is available, controllers that are also transiently optimal can be designed, but they will likely not be fully decentralized. In short, such optimal controllers violate the "plug-and-play" philosophy in microgrid operation [15].

5 Secondary Integral Control

The primary droop control (7) results in a generally nonzero stationary voltage drift given in (8) which has to be compensated by means of a secondary controller. In what follows, we investigate two secondary control strategies: a fully decentralized one and a distributed one.

5.1 Decentralized Integral Control

To compensate the steady-state drift (8), we augment every droop controller (7) with a local integral controller penalizing voltage drifts. The resulting PI controller is

$$I_i^S = I_i^* - C_i \dot{V}_i^S - p_i \tag{24a}$$
$$D_i \dot{p}_i = \dot{V}_i^S \tag{24b}$$

where p_i is an integral control variable, and $D_i > 0$ is a gain. Notice that (24) is a generalization of the PI droop controller (6), which reduces to the conventional DC droop control (5) in steady state. The decentralized integral controller (24) (and equivalently conventional DC droop controller (5)) successfully corrects for the steady-state voltage drifts but fails to recover the desired injections for load sharing and economic optimality. Fig. 5 shows an analog circuit realization of the decentralized integral controller (24). In a digital implementation, a micro-controller can be programmed to realize (24) based on source-current measurements.

Theorem 5.1 (Performance of decentralized integral control) Consider the closed-loop secondary-controlled microgrid (1) with the decentralized integral controller (24). Then the following statements hold:
(**1**) All source voltages $V_i^S(t)$ converge to stationary values without drift.
(**2**) The steady-state source injections do generally not achieve proportional load sharing (4).
(**3**) The steady-state source injections are generally not optimal with respect to the economic dispatch (18).

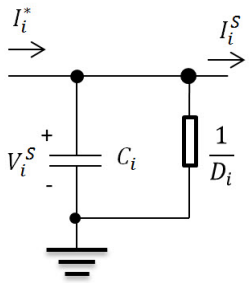

Fig. 5. Analog circuit realization of the integral controller (24) in the form (25) with zero initial conditions.

Proof 5.1 *The secondary controller* (24) *is identical to,*

$$I_i^S = -C_i\dot{V}_i^S + I_i^* - D_i^{-1}(V_i^S - V_i^S(0)) + p_i(0), \quad (25)$$

where $V_i^S(0)$ *and* $p_i(0)$ *are initial values of* V_i^S *and* p_i*, respectively. The closed-loop state space model is then obtained by combining the equation* (1) *and equation* (25)

$$\begin{bmatrix} C\dot{V}^S \\ 0 \end{bmatrix} = \begin{bmatrix} \hat{I}_S^* \\ I^L \end{bmatrix} - \begin{bmatrix} Y_{SS} & Y_{SL} \\ Y_{SL}^T & Y_{LL} \end{bmatrix} \begin{bmatrix} V^S \\ V^L \end{bmatrix} - \begin{bmatrix} D^{-1}V^S \\ 0 \end{bmatrix} \quad (26)$$

where $\hat{I}_S^* = I_S^* + D^{-1}(V^S(0) - p(0))$*.*

The associated Kron-reduced system is given by

$$C\dot{V}^S = -(\tilde{L} + D^{-1})V^S + \hat{I}, \quad (27)$$

where $D = \boldsymbol{diag}(D_1, ..., D_m)$ *and* $\hat{I} = \hat{I}_S^* - Y_{SL}Y_{LL}^{-1}I^L$*.*

Since $\tilde{L} \geq 0$ *and* $D^{-1} > 0$*, we have that* $\tilde{L} + D^{-1} > 0$*. Then according to Sylvester's Law of Inertia [19],* $-C^{-1}(\tilde{L} + D^{-1})$ *has strictly negative eigenvalues. Thus, with a constant vector* $C^{-1}\hat{I}$*, the voltage sources* V^S *converge to the asymptotically stable equilibrium* $V^S(\infty) = (\tilde{L} + D^{-1})^{-1}\hat{I}$*. This concludes the proof of statement (1).*

The closed loop (1) *and* (24) *is (after Kron reduction)*

$$\begin{bmatrix} C\dot{V}^S \\ CD\dot{p} \end{bmatrix} = \begin{bmatrix} \mathbf{I} & \mathbf{I} \\ \mathbf{I} & \mathbf{I} \end{bmatrix} \begin{bmatrix} -\tilde{L}V^S + \tilde{I} \\ -p \end{bmatrix}. \quad (28)$$

The matrix $\left[\begin{smallmatrix} \mathbf{I} & \mathbf{I} \\ \mathbf{I} & \mathbf{I} \end{smallmatrix}\right]$ *in* (28) *has nullspace* $[-x\ x]^T$ *for any* $x \in \mathbb{R}^m$*. Hence, the equilibria of* (28) *are for any* $\tau \in \mathbb{R}$

$$\begin{bmatrix} -\tilde{L}V^S + \tilde{I} \\ -p \end{bmatrix} = \tau \begin{bmatrix} -x \\ x \end{bmatrix}.$$

These equilibrium subspaces include (but are not equal to) the open-loop equilibria which are achieved for $x = \mathbb{0}_m$*.*

Observe that load sharing (4) *and economic optimality* (18) *can be achieved only for particular steady states satisfying* $x_i/C_i = x_j/C_j$ *or* $x_i\alpha_i = x_j\alpha_j$ *for all entries* i, j *of* x*, see* (19)*. However, these particular steady states are strict subsets of the equilibrium subspaces and can generally (for generic initial conditions) not be reached. This concludes the proofs of statement (2) and (3).* □

We conclude that the fully decentralized secondary integral controller (24) eliminates the voltage drift $\dot{v}_{\text{drift}}$, but it also obliterates the desired properties of proportional load sharing and economic optimality.

5.2 Distributed Consensus Filter

In the following, we focus on *distributed* secondary integral control strategies that are able to achieve the desired optimal injections at the requirement of communication.

The previous decentralized controllers (24) result in the stationary injection $I_i^S = I_i^* - p_i(t \to \infty)$ which depend on initial values, exogenous disturbances, and unknown load parameters and do not necessarily satisfy the optimality condition (20) of identical marginal costs. Hence, we propose the following *distributed consensus filter* to force an alignment of the marginal injection costs $\alpha_i p_i$:

$$I_i^S = I_i^* - C_i\dot{V}_i^S - p_i \quad (29a)$$

$$D_i\dot{p}_i = C_i\dot{V}^S - \sum\nolimits_{j=1}^{m} B_{ij}\left(\alpha_i p_i - \alpha_j p_j\right) \quad (29b)$$

where $D_i > 0$ and the terms $B_{ij} = B_{ji} \geq 0$ induce an undirected and connected communication graph among the sources $\mathcal{V}_s$. The consensus filter (29) resembles the distributed averaging PI (DAPI) controller proposed in [16], and it combines the integral action (24) together with a consensus flow [24]. At the price of requiring communication between the sources, the distributed consensus filter (29) achieves regulation of the voltage drifts while recovering the desired injections for proportional load sharing or economic optimality, respectively.

Theorem 5.2 (Performance of distributed consensus filter) Consider the closed-loop secondary-controlled microgrid (1) with the distributed consensus filter (29). Then the following statements hold:
(**1**) All source voltages $V_i^S(t)$ converge to stationary values without drift.
(**2**) The steady-state source injections achieve proportional load sharing (4) if the controller gains are chosen as in (9).
(**3**) The steady-state source injections are optimal with respect to the economic dispatch problem (18) if the controller gains are chosen as in (21).

The proof of Theorem 5.2 is presented in the Appendix. We conclude our analysis with a remark on the load voltages that were so far left out of the picture.

Remark 5.1 (Control of the load voltages) *In our analysis we focused on controlling the sources, and the load voltages V^L are determined as function of the source voltages (and thus the current injection setpoints I_i^* and corrections through primary/secondary control) by inverting the Kron reduction: $V^L = Y_{LL}^{-1}(I^L - Y_{SL}^T V^S)$. Clearly, if the loads are attached to controllable voltage (source) buses, then their voltages can be directly controlled. In the more general under-actuated case, we show in the following how a desirable load voltage profile can be guaranteed by scheduling the nominal source injections I_i^* accordingly. Consider the network balance equations* (1) *evaluated in steady state for $I^S = I^* - p^*$. Recall from [18] that any principal minor of the Laplacian Y is nonsingular (provided that the microgrid is connected). Thus, we can eliminate the source voltage V^S and obtain*

$$I^L + \bar{Y}(I^* - p^*) = \tilde{Y} V^L \,, \tag{30}$$

where $\tilde{Y} = Y_{LL} - Y_{SL} Y_{SS}^{-1} Y_{SL}^T$ is the reduced admittance matrix and $\bar{Y} = -Y_{SL}^T Y_{SS}^{-1}$. Equation (30) *relates the load bus voltages V^L and the source injections I^*, and it can be used to schedule the source injections I^* to achieve a desirable nominal load voltage profile V^L, e.g., by solving a feasibility problem subject to upper and lower bounds on the load voltages. To do so the network admittance matrix Y needs to be known as well as a forecast for the nominal load I^L and its worst-case deviations which can be mapped into the required secondary control action p^*.*

In such setup, a nominal operating point is scheduled offline based on a system model and a load forecast so that nominal voltage bounds are guaranteed, and the primary and secondary controllers compensate for deviations from the nominally forecasted load profile in real-time. □

6 Simulation Results

We illustrate the performance of our proposed controllers in a simulation scenario. We consider the microgrid displayed in Fig. 1, where $\mathcal{V}_S = \{a,\ b,\ c\}$ and $\mathcal{V}_L = \{d,\ e,\ f,\ g,\ h\}$. The microgrid is operating in islanded mode, and the dashed blue lines indicate the communication topology among the controllers in the distributed consensus filter (29). To achieve proportional load sharing, the droop coefficients C_i are chosen to be proportional to the source capacity $\bar{I}$ as in (9). At $t = 10s$ the initial load demand $I^L = [-1,\ -2,\ -3,\ -3,\ -2]^T$ changes instantaneously to $I^L = [-4,\ -0.5,\ -1.5,\ -5,\ -0.5]^T$. We investigate the transient and stationary behavior of the closed-loop system using different control strategies; see Fig. 6.

The simulation results using primary droop control (7) are shown in Fig. 6(a). The constant voltage drifts ($\dot{v}_{\text{drift}}$) are visible as nonzero and identical (in steady state) slopes in Fig. 6(a), and the load sharing ratios ($I_i^S/\bar{I}_i$) converge to the same steady-state value, i.e., the load is shared proportionally. Fig. 6(b) shows the simulation results using decentralized integral control (24).The source voltages converge to constant values without drifts, but the load sharing ratios do not converge to the same steady-state values. Additionally, the red injection in Fig. 6(b) exceeds the value 1, that is, the associated source injection exceeds its capacity. Moreover, the blue injection in Fig. 6(b) shows that, the current injection is negative at steady state, that is, the associated source should absorb (instead of supply) current, which reveals another disadvantage of decentralized integral control. The simulation results using the distributed consensus filter (29) are shown in Fig. 6(c). Observe that the source voltages converge to constant values without drifts, and the load sharing ratios converge to the same values. Hence, the voltage drifts are regulated and proportional load sharing is achieved. Finally, note the different scales in the plots which indicate a superior transient performance of the distributed consensus filter (29).

7 Conclusions

We proposed decentralized and distributed primary droop and secondary integral control strategies in DC microgrids. We analyzed the properties and limitations of these control strategies, and investigated their consistencies with tertiary-level objectives such as proportional load sharing and an economic dispatch among the generating units. This work is a first step towards establishing an operation architecture for DC microgrids. In our initial setup, we assumed constant current or constant impedance loads, and we considered purely resistive networks or networks with lines modeled by the resistive-capacitive Π-model. In ongoing and future work, we plan to study the robust performance in presence of transient stochastic disturbances as well as different network models including resistive-inductive-capacitive lines and constant power load models using the approximation proposed in [25].

8 Acknowledgements

The authors wish to thank A. Davoudi and M. Andreasson for their helpful comments and suggestions.

References

[1] J. Zhao and F. Drfler. Distributed control, load sharing, and dispatch in DC microgrids. In *American Control Conference*, 2015. To appear.

[2] J. M. Guerrero, J. C. Vasquez, J. Matas, L. G. de Vicuna, and M. Castilla. Hierarchical control of droop-controlled AC and DC microgrids–a general approach toward standardization. *IEEE Transactions on Industrial Electronics*, 58(1):158–172, 2011.

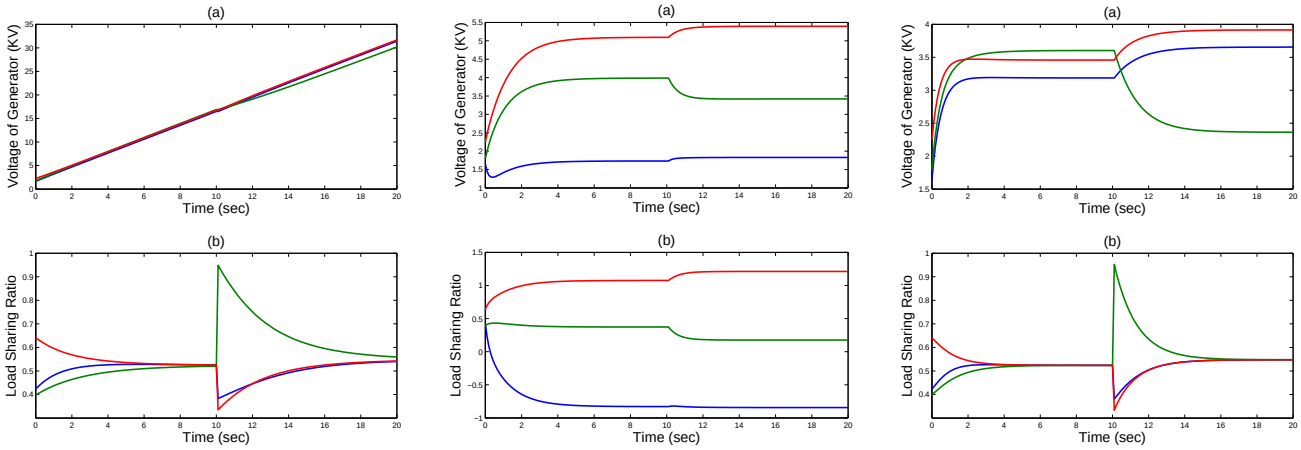

(a) Primary droop control (7). (b) Decentralized integral control (24). (c) Distributed consensus filter (29).

Fig. 6. Closed-loop performance of the microgrid under different control strategies

[3] D. Nilsson and A Sannino. Load modelling for steady-state and transient analysis of low-voltage dc systems. In *Industry Applications Conference, 2004. 39th IAS Annual Meeting. Conference Record of the 2004 IEEE*, volume 2, pages 774–780 vol.2, Oct 2004.

[4] Jackson John Justo, Francis Mwasilu, Ju Lee, and Jin-Woo Jung. Ac-microgrids versus dc-microgrids with distributed energy resources: A review. *Renewable and Sustainable Energy Reviews*, 24(0):387 – 405, 2013.

[5] Youichi Ito, Yang Zhongqing, and Hirofumi Akagi. Dc microgrid based distribution power generation system. In *Power Electronics and Motion Control Conference, 2004. IPEMC 2004. The 4th International*, volume 3, pages 1740–1745. IEEE, 2004.

[6] D. Salomonsson and A. Sannino. Low-voltage dc distribution system for commercial power systems with sensitive electronic loads. *Power Delivery, IEEE Transactions on*, 22(3):1620–1627, July 2007.

[7] Q. Shafiee, T. Dragicevic, J.C. Vasquez, and J.M. Guerrero. Modeling, stability analysis and active stabilization of multiple dc-microgrid clusters. In *Energy Conference (ENERGYCON), 2014 IEEE International*, pages 1284–1290, May 2014.

[8] Lie Xu and Dong Chen. Control and operation of a dc microgrid with variable generation and energy storage. *Power Delivery, IEEE Transactions on*, 26(4):2513–2522, 2011.

[9] J. W. Simpson-Porco, F. Drfler, and F. Bullo. On resistive networks of constant power devices. *IEEE Transactions on Circuits and Systems II: Express Briefs*, 2015. To appear. Available at http://arxiv.org/pdf/1503.04769v1.pdf.

[10] V. Nasirian, S. Moayedi, A. Davoudi, and F.L. Lewis. Distributed cooperative control of dc microgrids. *Power Electronics, IEEE Transactions on*, 30(4):2288–2303, April 2015.

[11] M. Andreasson, D. V. Dimarogonas, H. Sandberg, and K. H. Johansson. Control of MTDC Transmission Systems under Local Information. *ArXiv e-prints*, June 2014.

[12] M. Tucci, S. Riverso, J. C. Vasquez, J. M. Guerrero, and G. Ferrari-Trecate. A decentralized scalable approach to voltage control of DC islanded microgrids. *ArXiv e-prints*, March 2015.

[13] T. Morstyn, B. Hredzak, G.D. Demetriades, and V.G. Agelidis. Unified distributed control for dc microgrid operating modes. *Power Systems, IEEE Transactions on*, PP(99):1–11, 2015.

[14] D. Zonetti, R. Ortega, and A. Benchaib. Modeling and Control of High-Voltage Direct-Current Transmission Systems: From Theory to Practice and Back. *ArXiv e-prints*, June 2014.

[15] F. Dörfler, J. Simpson-Porco, and F. Bullo. Breaking the Hierarchy: Distributed Control & Economic Optimality in Microgrids. *ArXiv e-prints*, January 2014.

[16] J. W. Simpson-Porco, F. Dörfler, and F. Bullo. Synchronization and power sharing for droop-controlled inverters in islanded microgrids. *Automatica*, 49(9):2603–2611, 2013.

[17] P. Karlsson and J. Svensson. Dc bus voltage control for a distributed power system. *Power Electronics, IEEE Transactions on*, 18(6):1405–1412, Nov 2003.

[18] F. Dörfler and F. Bullo. Kron reduction of graphs with applications to electrical networks. *IEEE Transactions on Circuits and Systems I: Regular Papers*, 60(1):150–163, 2013.

[19] Alexander Ostrowski and Hans Schneider. Some theorems on the inertia of general matrices. *Journal of Mathematical analysis and applications*, 4(1):72–84, 1962.

[20] P. Kundur. *Power System Stability and Control*. McGraw-Hill, 1994.

[21] R. A. Horn and C. R. Johnson. *Matrix Analysis*. Cambridge University Press, 1985.

[22] Fuzhen Zhang. *The Schur complement and its applications*, volume 4. Springer, 2006.

[23] S. Boyd and L. Vandenberghe. *Convex Optimization*. Cambridge University Press, 2004.

[24] F. Bullo, J. Cortés, and S. Martínez. *Distributed Control of Robotic Networks*. Princeton University Press, 2009.

[25] B. Gentile, J. W. Simpson-Porco, F. Drfler, S. Zampieri, and F. Bullo. On reactive power flow and voltage stability in microgrids. In *American Control Conference*, pages 759–764, Portland, OR, June 2014.

[26] Steven H Weintraub. A guide to advanced linear algebra. (44), 2011.

A Proof of Theorem 5.2

Proof A.1 *The closed-loop state space model* (1), (29) *is*

$$\begin{bmatrix} C\dot{V}^S \\ \mathbf{0_{n-m}} \\ D\dot{p} \end{bmatrix} = \begin{bmatrix} I_S^* \\ I^L \\ I_S^* \end{bmatrix} - \begin{bmatrix} Y_{SS} & Y_{SL} & \mathbf{I_m} \\ Y_{SL}^T & Y_{LL} & \mathbf{0_{n-m}} \\ Y_{SS} & Y_{SL} & L_cC^{-1} + \mathbf{I_m} \end{bmatrix} \begin{bmatrix} V^S \\ V^L \\ p \end{bmatrix}$$

where $p = [p_1 \ \dots \ p_m]^T$, *and* L_c *is the Laplacian matrix induced by the communication graph with weights* $B_{ij} = B_{ji} \geq 0$. *After Kron-reduction, the reduced system is*

$$\begin{bmatrix} C\dot{V}^S \\ D\dot{p} \end{bmatrix} = - \begin{bmatrix} \tilde{L} & \mathbf{I_m} \\ \tilde{L} & (\mathbf{I_m} + L_cC^{-1}) \end{bmatrix} \begin{bmatrix} V^S \\ p \end{bmatrix} + \begin{bmatrix} \tilde{I} \\ \tilde{I} \end{bmatrix} \quad \text{(A.1)}$$

Let $p^* = C\mathbb{1}\dot{v}_{\text{drift}} = C\mathbb{1}\mathbb{1}^T\tilde{I}/\sum_{i=1}^m C_i$ *then* $\mathbb{1}_m^T(\tilde{I} - p^*) = 0$. *It follows that* $(\tilde{I} - p^*)$ *is in the range of* $\tilde{L}$ *and there is* V_S^* *so that* $-\tilde{L}V_S^* - p^* + \tilde{I} = \mathbb{0}_m$. *Let* $\tilde{V}_S = V^S - V_S^*$ *and* $\tilde{P} = p - p^*$, *then system* (A.1) *becomes*

$$\begin{aligned} \begin{bmatrix} \dot{\tilde{V}}_S \\ \dot{\tilde{P}} \end{bmatrix} &= - \begin{bmatrix} C^{-1}\tilde{L} & C^{-1}\mathbf{I_m} \\ D^{-1}\tilde{L} & D^{-1}(\mathbf{I_m} + L_cC^{-1}) \end{bmatrix} \begin{bmatrix} \tilde{V}_S \\ \tilde{P} \end{bmatrix} \quad \text{(A.2)} \\ &= - \begin{bmatrix} \mathbf{I} & \mathbb{0} \\ \mathbb{0} & D^{-1} \end{bmatrix} \begin{bmatrix} C^{-1} & \mathbf{I} \\ \mathbf{I} & C + L_c \end{bmatrix} \begin{bmatrix} \tilde{L} & \mathbb{0} \\ \mathbb{0} & C^{-1} \end{bmatrix} \begin{bmatrix} \tilde{V}_S \\ \tilde{P} \end{bmatrix}, \end{aligned}$$

where $\mathbb{0}$ *and* $\mathbf{I}$ *denote zero and identity matrices of appropriate dimension. The characteristic equation of the negative system matrix in* (A.2) *reads as*

$$\begin{aligned} &\det\left(\lambda\mathbf{I} - \begin{bmatrix} \mathbf{I} & \mathbb{0} \\ \mathbb{0} & D^{-1} \end{bmatrix} \begin{bmatrix} C^{-1} & \mathbf{I} \\ \mathbf{I} & C + L_c \end{bmatrix} \begin{bmatrix} \tilde{L} & \mathbb{0} \\ \mathbb{0} & C^{-1} \end{bmatrix}\right) \\ &= \det\left(\begin{bmatrix} \mathbf{I} & \mathbb{0} \\ \mathbb{0} & D^{-1} \end{bmatrix}\right) \det\left(\lambda \begin{bmatrix} \mathbf{I} & \mathbb{0} \\ \mathbb{0} & D \end{bmatrix} - \begin{bmatrix} C^{-1} & \mathbf{I} \\ \mathbf{I} & C + L_c \end{bmatrix} \begin{bmatrix} \tilde{L} & \mathbb{0} \\ \mathbb{0} & C^{-1} \end{bmatrix}\right) \\ &= \det\left(\lambda \begin{bmatrix} \mathbf{I} & \mathbb{0} \\ \mathbb{0} & D \end{bmatrix} - \begin{bmatrix} C^{-1} & \mathbf{I} \\ \mathbf{I} & C + L_c \end{bmatrix} \begin{bmatrix} \tilde{L} & \mathbb{0} \\ \mathbb{0} & C^{-1} \end{bmatrix}\right) \det\left(\begin{bmatrix} \mathbf{I} & \mathbb{0} \\ \mathbb{0} & D^{-1} \end{bmatrix}\right) \\ &= \det\left(\lambda\mathbf{I} - \begin{bmatrix} C^{-1} & \mathbf{I} \\ \mathbf{I} & C + L_c \end{bmatrix} \begin{bmatrix} \tilde{L} & \mathbb{0} \\ \mathbb{0} & C^{-1}D^{-1} \end{bmatrix}\right). \end{aligned}$$

The matrix $\begin{bmatrix} \tilde{L} & \mathbb{0} \\ \mathbb{0} & C^{-1}D^{-1} \end{bmatrix}$ *is positive semidefinite with one zero eigenvalue and corresponding eigenvector* $\begin{bmatrix} \mathbb{1}_m^T & \mathbb{0} \end{bmatrix}^T$, *and* $\begin{bmatrix} C^{-1} & \mathbf{I} \\ \mathbf{I} & C+L_c \end{bmatrix}$ *is positive semidefinite. Let* $\sigma > 0$, *and consider the perturbed matrix* $\begin{bmatrix} C^{-1} & \mathbf{I} \\ \mathbf{I} & C+L_c+\sigma\mathbf{I} \end{bmatrix}$, *which is positive definite. According to Sylvester's Law of Inertia [26], the matrix* $\begin{bmatrix} C^{-1} & \mathbf{I} \\ \mathbf{I} & C+L_c+\sigma\mathbf{I} \end{bmatrix} \begin{bmatrix} \tilde{L} & \mathbb{0} \\ \mathbb{0} & C^{-1}D^{-1} \end{bmatrix}$ *has one zero eigenvalue, and all other eigenvalues are positive. Recall that the eigenvalues of a matrix are continuous functions of the matrix elements (via the characteristic equation). Since there is only a single zero and* $m-1$ *positive eigenvalues for any* $\sigma > 0$, *the number of zero eigenvalues can either increase or remain unchanged as* $\sigma \downarrow 0$. *For* $\sigma = 0$, $\mathbb{0}$ *and* $[\mathbb{1}_m \ \mathbb{0}]^T$ *are an eigenvalue and eigenvector pair. Also, the range space of* $\begin{bmatrix} \tilde{L} & \mathbb{0} \\ \mathbb{0} & C^{-1}D^{-1} \end{bmatrix}$ *and the null space of* $\begin{bmatrix} C^{-1} & \mathbf{I} \\ \mathbf{I} & C+L_c \end{bmatrix}$ *do not coincide. Thus,* $\begin{bmatrix} \mathbb{1}_m^T & \mathbb{0}_m \end{bmatrix}^T$ *is the only eigenvector associated to the zero eigenvalue of the system* (A.2). *Hence, there is only one zero eigenvalue and all the other eigenvalues are positive.*

We conclude that the solutions of the system (A.2) *converge to* $[\kappa\mathbb{1}_m \ \mathbb{0}_m]^T$, *where* $\kappa \in \mathbb{R}$. *Equivalently,* $\begin{bmatrix} V^S & p \end{bmatrix}^T$ *converges to the constant vector* $\begin{bmatrix} V_S^{*T} + \kappa\mathbb{1}_m^T & p^* \end{bmatrix}^T$. *Therefore, at steady state,* $\dot{V}_S(\infty) = 0$. *This proves statement (1).*

To prove statements (2) and (3), we write (A.1) *as*

$$\begin{bmatrix} C\dot{V}^S \\ D\dot{p} \end{bmatrix} = \begin{bmatrix} \mathbf{I} & \mathbf{I} \\ \mathbf{I} & \mathbf{I} + L_cC^{-1} \end{bmatrix} \begin{bmatrix} -\tilde{L}V^S + \tilde{I} \\ -p \end{bmatrix}.$$

The matrix $\begin{bmatrix} \mathbf{I} & \mathbf{I} \\ \mathbf{I} & \mathbf{I}+L_cC^{-1} \end{bmatrix}$ *in the above equation has nullspace* $[C\mathbb{1} \ -C\mathbb{1}]^T$, *and the equilibria of* (A.1) *are*

$$\begin{bmatrix} -\tilde{L}V^S + \tilde{I} \\ -p \end{bmatrix} = \tau \begin{bmatrix} C\mathbb{1} \\ -C\mathbb{1} \end{bmatrix}$$

for some $\tau \in \mathbb{R}$. *We multiply the equation* $-\tilde{L}V^S + \tilde{I} = \tau C\mathbb{1}_m$ *by* $\mathbb{1}_m^T$ *on both sides: the first term of left-hand side equals* $-\mathbb{1}_m^T\tilde{L}V^S = 0$, *the second term of the left-hand side equals* $\mathbb{1}_m^T\tilde{I} = \mathbb{1}_m^T(I_S^* - Y_{SL}Y_{LL}^{-1}I^L) = \mathbb{1}_m^TI_S^* + \mathbb{1}_{n-m}^TI^L$ *and the right-hand side equals* $\mathbb{1}_m^S\tau C\mathbb{1}_m = \tau\sum_{i\in\mathcal{V}_S} C_i$. *Thus,* $\tau = (\mathbb{1}_m^TI_S^* + \mathbb{1}_{n-m}^TI^L)/(\sum_{i\in\mathcal{V}_S} C_i)$ *and* $p = \tau C\mathbb{1}_m$. *We conclude that the steady-state injections of sources are determined by* $I^S(\infty) = I^* - p = I^* - C\tau\mathbb{1}_m$, *which equals the steady-state injections of the primary control system* (1) *and* (7). *Therefore, statements (2) and (3) in Theorem 5.2 follow from statement (2) of Theorem 3.1 and Corollary 4.1.* □